Evaluation of pancreatic steatosis prevalence and anthropometric measurements using non-contrast computed tomography

Ural Koç, Onur Taydaş

Department of Radiology, Erzincan Mengucek Gazi Training and Research Hospital, Erzincan, Turkey

Cite this article as: *Koç U, Taydaş O. Evaluation of pancreatic steatosis prevalence and anthropometric measurements using non-contrast computed tomography. Turk J Gastroenterol 2020; 31(9): 640-8.*

ABSTRACT

Background/Aims: *Pancreatic steatosis (PS) is a subject of current interest, and its prevalence has been reported to range from 16.1% to 30.7% using various radiological methods. This study aimed to evaluate PS prevalence using non-contrast computed tomography (CT).*

Materials and Methods: *The non-contrast CT scans taken in 2016 and 2017 in our hospital were retrospectively screened. A total of 637 patients (320 men and 317 women) were included in the study. The number measurements on the CT were performed from 3 anatomic regions of the pancreas using regions of interest (ROI) of approximately 1 cm^2. The cases with a <0.7 ratio of the pancreatic over splenic CT number were accepted as quantitatively steatosis positive. Anthropometric evaluations were undertaken by determining various parameters defined on CT.*

Results: *PS was determined visually in 30.6% of the men and 29% of the women and quantitatively in 32.8% and 30.6%, respectively. A positive agreement was determined between the quantitative and visual evaluations of steatosis (Cohen's kappa coefficient=0.587, p<0.001). Although PS was seen to be mostly diffuse, the tail region of the pancreas was determined to be the area with the most steatosis.*

Conclusion: *PS is usually overlooked in radiology practice, but it has a clinical presentation with an insignificant prevalence. Current radiological methods are adequate in the evaluation of PS. Determination of the cutoff values for various criteria on non-contrast CT can provide more objective evaluations.*

Keywords: *Pancreas, tomography, radiology, prevalence*

INTRODUCTION

Pancreatic steatosis (PS), which is the accumulation of lipid in the pancreas, was first defined in the early 20th century by Ogilvie in a cadaver study (1). In the second half of that century, Olsen and Stamm demonstrated the relationship of PS with age, atherosclerosis, and diabetes in autopsy studies (2, 3). Obesity, which has become a global epidemic, is related to type 2 diabetes, metabolic syndrome, nonalcoholic fatty liver disease (NAFLD), and cardiovascular diseases. This process leads to the ectopic accumulation of triglycerides in nonadipose tissue, such as in the liver, skeletal muscle, pancreatic cells, and heart and results in multisystem problems (4). Although age and obesity are at the forefront in the etiology of PS, various other factors, including alcohol consumption, diabetes, and viral infections, have also been implicated (4). Studies examining the clinical reflection of PS reported increased severity of pancreatitis associated with PS, which led to endocrine or exocrine deficiencies or impairments (5). Hori et al. (6) reported that the amount of PS was an independent risk factor for the development of pancreatic cancer. Furthermore, PS has been shown to lead to the development of postoperative pancreatic fistula (POPF) (7). There are no clinical or laboratory biomarkers for PS, and the findings of radiological modalities that indicate PS are usually overlooked.

Cross-sectional imaging techniques, such as proton density fat fraction (PDFF) magnetic resonance imaging (MRI) or computed tomography (CT), are commonly used for liver fat quantification (8-10). Recent studies have demonstrated that MRI PDFF and non-contrast CT linearly correlated as non-invasive methods for quantification of fat in the liver (9, 10). These methods have been also gained interest in the field of pancreatology in the recent literature (11-13). Clinical results related to fatty pancreas are controversial, unlike fatty liver disease. Recent literature shows conflicting publications concerning whether PS is associated with pancreatic endocrine and/or exocrine function. For example, Tahtacı et al. (14)

Corresponding Author: ***Ural Koç; dr_uralkoc@hotmail.com***
Received: ***May 29, 2019*** *Accepted:* ***March 21, 2020***

DOI: ***10.5152/tjg.2020.19434***

observed on MRI that fatty pancreas could result in pancreatic exocrine impairment. However, Miyake et al. (15) reported that fatty pancreas did not result in pancreatic exocrine impairment, but there were signs of endocrine impairment on CT. A previous study of patients with NAFLD reported that nonalcoholic fatty pancreas disease was seen more often in patients with NAFLD, with an increased risk of metabolic syndrome (16). Recent studies estimated NAFLD prevalence to be over 30% in Turkey and 25% globally (17, 18). To the best of our knowledge, pancreatic steatosis prevalence in Turkey has not been previously reported in the literature.

This study aimed to evaluate PS prevalence according to sex and age in an extensive sample using non-contrast CT.

MATERIALS AND METHODS

Study Protocol and Patients

The non-contrast CT scans of the patients referred to the Radiology Clinic of Erzincan Mengucek Gazi Training and Research Hospital between January 2016 and December 2017 were retrospectively screened. A total of 637 patients (age range, 18–91 years) were included in the study. These patients had been initially referred to our clinic for CT owing to suspicion of stones or adrenal lesions or complaint of nonspecific abdominal pain, but they were also determined to have no positive findings and thus were treated with simple medication.

The patients were excluded from the study if their medical records revealed a history of pancreatic surgery, recurrent acute pancreatitis, chronic pancreatitis, autoimmune pancreatitis, pancreatic lesions, blood transfusion, hemochromatosis, malignancy, chemotherapy, or iron overload. The approval for the study was granted by the local ethics committee (13.02.2018/19/15), and all procedures were applied in accordance with the Helsinki Declaration. Informed consent was waived because of the retrospective nature of the study.

MAIN POINTS

- *Pancreatic steatosis (PS) can be evaluated by non-invasive cross-sectional imaging techniques.*
- *Computed tomography (CT) provides both quantitative and qualitative information for the evaluation of PS and anthropometric evaluations.*
- *PS was determined quantitatively in 32.8% of the men and 30.6% of the women via non-contrast CT.*
- *Prevalance rate of PS in our study sample is almost similar with NAFLD prevalance rate in Turkey.*

Imaging Technique

The patients underwent abdominopelvic CT using a 16-detector CT scanner (Somatom Emotion 16, Siemens Medical Systems, Germany). The region between the level of the upper diaphragm and ischial tubercles was included in the area of the scan. No intravenous or oral contrast material was used for CT examinations. The CT acquisition parameters were as follows: tube voltage, 130 kV; effective mAs, 110; slice thickness, 5 mm; collimation, 16 mm×1.2 mm; pitch, 0.8; and reconstruction increment, 1.5 mm; automatic tube current modulation, off; reconstruction method, filtered back projection; reconstruction kernel, B41s; and no usage of iterative reconstruction algorithm. The CT scanner was calibrated daily for quality control of CT number measurements. The kilovolt settings were kept constant owing to the effect on mean CT number measurements.

Evaluation of PS

CT number (Hounsfield Unit) measurements were performed in the head-neck, body, and tail sections of the pancreas from regions of interest (ROI) of approximately 1cm^2 on non-contrast CT images by 2 experienced radiologists (UK and OT, with 7 and 6 years of experience in abdominal CT, respectively) in the same session. The results were recorded according to consensus (Figure 1). When defining the ROI, the vessel traces, calcifications, extrapancreatic fat tissue area, and pancreatic duct traces were not included. A quantitative evaluation was undertaken by dividing the mean ROI values

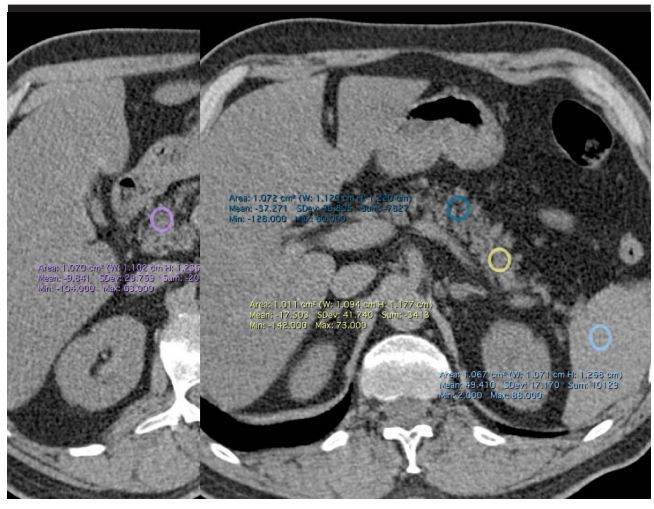

Figure 1. Measurements performed in the head-neck, body, and tail sections of the pancreas and spleen from regions of interest of approximately 1 cm^2 on non-contrast axial computed tomography images.

measured from 3 anatomic regions (head-neck, body, and tail) by the ROI CT number values measured from the spleen on the same slices. A ratio of <0.7 was accepted as PS (19). A visual evaluation was also applied to determine the presence or absence of PS, and the level of PS was graded as none to mild, moderate, or severe. On axial images of non-contrast CT, the grade of PS was visually analyzed depending on a 3-point scale (none to mild:0%–33%, moderate:34%–66%, and severe:67%–100%). Pancreatic atrophy, short pancreas, and pancreatic calcification findings were also recorded. The length of the pancreas was visually evaluated as short if the pancreatic tail did not end near the spleen. Pancreatic atrophy was visually evaluated as fat accumulation in the pancreas and a decrease in the size of pancreatic parenchyma (20, 21).

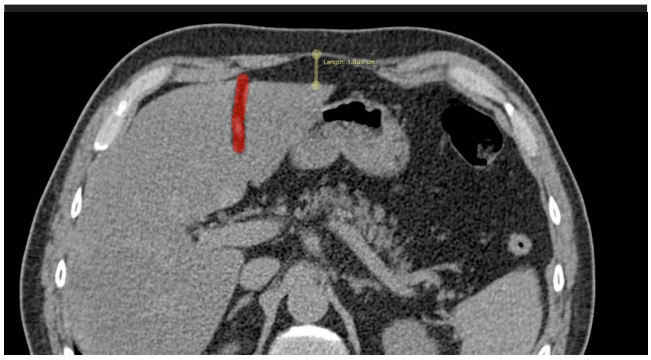

Figure 2. Intra-abdominal fat tissue measurements in the axial planes at the falciform ligament level (shown in red).

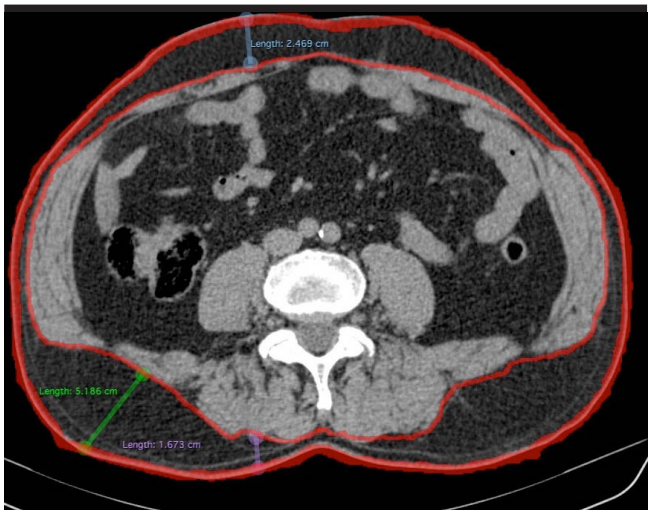

Figure 3. Measurements of the abdominal anterior-posterior diameter, abdominal transverse diameter, abdominal circumference (outer red circle), subcutaneous fat tissue area (between thick and thin red circle), and anterior (blue), posterior (purple) and posterolateral (green) subcutaneous fat tissue thicknesses at the peri-umbilical level.

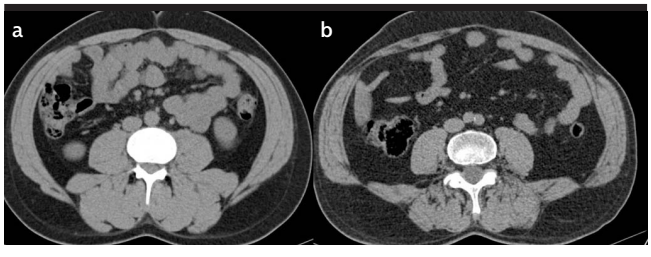

Figure 4. a, b. Visual evaluation of the visceral fat layer as mild (a) and moderate to severe (b).

Anthropometric Measurements

The abdominal anterior-posterior (AP) diameter, abdominal transverse diameter, abdominal circumference, subcutaneous fat tissue area, and anterior, posterior, and posterolateral subcutaneous fat tissue thickness were measured at the peri-umbilical level, and intra-abdominal fat tissue measurements were performed in the axial planes at the falciform ligament level by the same radiologists involved in the PS evaluation (Figures 2 and 3). The visceral fat layer was visually evaluated on a 2-point scale as mild and moderate to severe (Figure 4). The presence or absence of aortic and large vessel calcifications was also noted.

Statistical Analysis

The conformity of the variables to normal distribution was assessed using the Kolmogorov-Smirnov test. Continuous data were expressed as mean±standard deviation if they conformed to normal distribution and as median (minimum-maximum) values if the distribution was not normal. In the comparison of the paired groups, chi-squared and Fisher's exact tests were applied to the nominal and ordinal data. The independent t-test or the Mann–Whitney U test was applied to numerical data according to the conformity to normal distribution. In multiple comparisons, analysis of varianceor Kruskal-Wallis test was employed depending on the normality of distribution. The correlations between the nominal and numerical data were examined using the Spearman's correlation test. In addition, the Cohen's kappa coefficient was calculated to determine intra-assessment reliability. To evaluate independent risk factors, binary logistic regression analysis was used. A value of $p<0.05$ was accepted as statistically significant. The Statistical Package for the Social Sciences (SPSS) software version 21 for Windows (IBM Corp.; Armonk, NY, USA) was used to performthe statistical analyses.

RESULTS

The evaluation was performed in 637 patients, including 320 men with a mean age of 48 (range, 18–91) years and 317 women with a mean age of 48 (range, 18–88) years (Table 1).

No statistically significant difference was determined between the sexes with respect to mean ROI CT number values of the pancreatic head-neck, body, and tail sections or the spleen. In the visual evaluation, PS was observed in 30.6% of men and 29% of women. In the quantitative evaluation obtained by dividing the mean CT number values of the pancreatic head-neck, body, and tail sections by the mean CT number value of the spleen, PS was determined in 32.8% of menand 30.6% of women. Visual assessment graded the steatosis as none to mild in 92.2%, moderate in 7.5%, and severe in 0.3% formen and 90.5%, 7.3% and 2.2%, respectively, for women (p=0.112) (Table 1).

When the pancreatic regions were evaluated separately, the rate of steatosis was 20% in the head-neck region, 25.9% in the body section, and 29.7% in the tail section for men, and 18.3%, 22.7%, and 24.6%, respectively, for women. Furthermore, steatosis was determined in a single anatomic region in 8.4%, 2 anatomic regions in 5.9%, and 3 anatomic regions in 18.4% of men. For women, steatosis was determined in a single anatomic region in 10.4%, 2 anatomic regions in 5.4%, and 3 anatomic regions in 14.8%. No statistically significant difference was determined between the sexes in both the visual and quantitative evaluations (p=0.658 and p=0.548, respectively).

In the anthropometric evaluations, a statistically significant difference was determined between the sexes in terms of the AP abdominal diameter, transverse abdominal diameter, and abdominal circumference, and anterior, posterior, and posterolateral subcutaneous fat diameter and subcutaneous fat area (Table 1). However, there was no statistically significant difference between the 2 groups concerning the intra-abdominal fat diameter (p=0.107).

In the visual evaluation of the visceral fat layer, 77.8% of men and 74.8% of women were evaluated as moderate to severe (p=0.366). No statistically significant difference was determined between the sexes in relation to aortic and large vessel calcifications, pancreatic atrophy, presence of short pancreas, and pancreatic calcification (Table 2).

Table 1. Demographic data, CT number values of 3 anatomic regions of the pancreas, anthropometric CT measurements, and other parameters by sex.

Parameters	Men (n=320)	Women (n=317)	p
Age (years)	48 (18:91)	48 (18:88)	0.606
Pancreatic head-neck CT number (HU)	41 (−54:57)	41 (−69:59)	0.315
Pancreatic body CT number (HU)	40 (−39:59)	41 (−81:57)	0.059
Pancreatic tail CT number (HU)	39 (−67:53)	40 (−84:57)	0.085
Spleen CT number (HU)	46 (30:56)	46 (32:60)	0.138
Anterior-posterior abdominal diameter (mm)	247 (146:360)	228 (128:364)	<0.001
Transverse abdominal diameter (mm)	327.5 (216:430)	317 (205:467)	0.009
Abdominal circumference (mm)	982.5 (599:1387)	945 (601:1316)	<0.001
Anterior subcutaneous fat diameter (mm)	13 (2:48)	24 (4:55)	<0.001
Posterior subcutaneous fat diameter (mm)	10 (1:39)	15 (1:61)	<0.001
Posterolateral subcutaneous fat diameter (mm)	12 (2:47)	23 (3:80)	<0.001
Intra-abdominal fat diameter (mm)	11 (1:36)	11 (1:25)	0.107
Subcutaneous fat area (mm^2)	10,661 (1737:37923)	16,662 (1687:58246)	<0.001
Visual pancreatic steatosis grade			0.112
None–mild, n (%)	295 (92.2)	287 (90.5)	
Moderate, n (%)	24 (7.5)	23 (7.3)	
Severe, n (%)	1 (0.3)	7 (2.2)	
Visual visceral fat assessment			0.366
Mild, n (%)	71 (22.2)	80 (25.2)	
Moderate-severe, n (%)	249 (77.8)	237 (74.8)	
Aortic and great vessel calcification, n (%)	160 (50)	136 (42.9)	0.073
Pancreatic atrophy, n (%)	51 (15.9)	42 (13.2)	0.337
Short pancreas, n (%)	16 (5)	26 (8.2)	0.103
Pancreatic calcification, n (%)	1 (0.3)	2 (0.6)	0.623

CT: Computed tomography; HU: Hounsfield unit; n: Number of cases; %: Frequency; mm: Millimeter; mm2: Millimeter square.
Numeric values were represented as median (minimum:maximum), while categoric and nominal values were number (frequency).

When the patients were separated into age groups, no statistically significant difference was determined between the groups in terms of the CT number measurements (excluding the spleen), pancreas-spleen CT num-

Table 2. Visual steatosis, quantitative steatosis, pancreatic atrophy, visual visceral fat assessments, and large vessel calcification frequencies by sex (n= number of cases; %= frequency values for each age group; intra-group=same sex; inter-group=different sexes).

	Visual pancreatic steatosis (%)	Quantitative steatosis (%)	Pancreatic atrophy (%)	Visual visceral fat assessment (moderate-severe) (%)	Aortic and great vessels calcification (%)
Men vs.women (n=320 vs. 317)	30.6 vs. 29	32.8 vs. 30.6	15.9 vs. 13.2	77.8 vs. 74.8	50 vs. 42.9
18–29 years (n=64) vs. (n=54)	3.1 vs. 5.6	6.3 vs. 1.9	1.6 vs. 1.9	44.2 vs. 40.7	0 vs. 0
30–39 years (n=50) vs. (n=56)	6 vs. 7.1	8 vs. 7.1	6 vs. 0	76 vs. 50	10 vs. 7.1
40–49 years (n=52) vs. (n=51)	36.5 vs. 19.6	26.9 vs. 11.8	11.5 vs. 2	94.2 vs. 76.5	55.8 vs. 29.4
50–59 years (n=53) vs. (n=55)	37.7 vs. 32.7	43.4 vs. 40	32.1 vs. 21.8	90.6 vs. 92.7	67.9 vs. 61.8
60–69 years (n=51) vs.(n=52)	52.9 vs. 48.1	52.9 vs. 53.8	21.6 vs. 17.3	84.3 vs. 98.1	82.4 vs. 71.2
70 + years (n=50) vs. (n=49)	54 vs. 65.3	66 vs. 73.5	26 vs. 38.8	88 vs. 93.9	96 vs. 93.9
p (intra-group)	<0.001	<0.001	<0.001	<0.001	<0.001
p (inter-group)	0.658	0.548	0.337	0.366	0.073

Table 3. CT number values of 3 anatomic regions of the pancreas, anthropometric CT measurements, and other parameters of men according to age groups. Numeric values (HU, mm, mm^2) were represented as median (minimum:maximum).

Men (age groups)	18–29 years (n=64)	30–39 years (n=50)	40–49 years (n=52)	50–59 years (n=53)	60–69 years (n=51)	70 + years (n=50)	p
Pancreatic head-neck CT number (HU)	47 (13:54)	44 (−49:52)	40.5 (−3:47)	38 (0:54)	36 (−23:57)	33 (−54:50)	<0.001
Pancreatic body CT number (HU)	45 (9:59)	43 (−39:50)	39.5 (−21:50)	36 (−13:50)	33 (−34:52)	27 (−39:53)	<0.001
Pancreatic tail CT number (HU)	44 (11:53)	42 (−30:50)	37 (−3:48)	35 (−19:51)	34 (−30:49)	27.5 (−67:51)	<0.001
Spleen CT number (HU)	48 (35:56)	47 (36:56)	46 (38:52)	45 (30:54)	46 (37:54)	45.5 (38:56)	0.055
Anterior-posterior abdominal diameter (mm)	210 (175:313)	237.5 (180:323)	265.5 (192:360)	257 (146:332)	258 (170:329)	249.5 (181:312)	<0.001
Transverse abdominal diameter (mm)	295 (225:401)	322.5 (222:372)	336 (281:430)	335 (216:423)	340 (275:429)	334.5 (252:426)	<0.001
Abdominal circumference (mm)	878 (745:1157)	952 (728:1134)	1018.5 (858:1387)	1024 (599:1287)	1015 (788:1276)	1016 (713:1248)	<0.001
Anterior subcutaneous fat diameter (mm)	8.5 (2:37)	12 (4:32)	15 (3:32)	14 (3:24)	14 (4:29)	12.5 (5:48)	<0.001
Posterior subcutaneous fat diameter (mm)	8 (2:28)	10 (3:28)	13 (4:29)	11(2:25)	11 (3:39)	11 (1:31)	<0.001
Posterolateral subcutaneous fat diameter (mm)	8 (3:34)	11.5 (3:45)	13 (4:42)	13 (3:31)	14 (5:40)	13 (2:47)	<0.001
Intra-abdominal fat diameter (mm)	7 (1:20)	11 (3:21)	12.5 (2:24)	11 (5:20)	11 (2:25)	10 (2:36)	<0.001
Subcutaneous fat area (mm^2)	7076.5 (2451: 29478)	8966.5 (2345: 25333)	12335.5 (2654: 26441)	11095 (1737: 24268)	13363 (3188: 33421)	11526 (1737: 37923)	<0.001

CT: Computed tomography; HU: Hounsfield unit; mm: Millimeter; mm^2: Millimeter square

Table 4. CT number values of 3 anatomic regions of the pancreas, anthropometric CT measurements, and other parameters of women according to age groups. Numeric values (HU, mm, mm^2) were represented as median (minimum:maximum).

Women (Age groups)	18–29 years (n=54)	30–39 years (n=56)	40–49 years (n=51)	50–59 years (n=55)	60–69 years (n=52)	70 + years (n=49)	p
Pancreatic head-neck CT number (HU)	47 (34:59)	44.5 (22:56)	43 (−5:53)	40 (−35:57)	36 (7:50)	31 (−69:51)	<0.001
Pancreatic body CT number (HU)	46 (33:57)	45 (28:54)	42 (26:51)	40 (−66:51)	32.5 (−27:47)	26 (−81:49)	<0.001
Pancreatic tail CT number (HU)	44 (33:52)	44 (30:57)	42 (26:48)	39 (−81:52)	31 (−29:47)	28 (−84:46)	<0.001
Spleen CT number (HU)	47 (32:59)	46 (34:53)	46 (34:55)	46 (35:60)	44 (33:55)	46 (36:58)	0.082
Anterior-posterior abdominal diameter (mm)	193 (128:338)	207.5 (169:341)	233 (149:311)	247 (155:364)	244 (158:331)	258 (176:318)	<0.001
Transverse abdominal diameter (mm)	281 (205:417)	292.5 (237:419)	330 (263:390)	333 (231:441)	343.5 (258:409)	345 (234:467)	<0.001
Abdominal circumference (mm)	821.5 (601:1282)	865.5 (712:1153)	973 (761:1216)	986 (660:1316)	996.5 (707:1227)	1035 (774:1220)	<0.001
Anterior subcutaneous fat diameter (mm)	16 (4:48)	21 (4:39)	28 (7:42)	26 (10:48)	24 (11:42)	25 (6:55)	<0.001
Posterior subcutaneous fat diameter (mm)	9 (2:49)	10.5 (2:32)	16 (1:61)	19 (3:42)	19.5 (6:51)	16 (6:53)	<0.001
Posterolateral subcutaneous fat diameter (mm)	14 (3:56)	23 (3:66)	26 (8:72)	22 (9:50)	26.5 (11:58)	24 (5:80)	<0.001
Intra-abdominal fat diameter (mm)	9 (3:20)	10 (4:17)	13 (4:25)	11 (1:22)	12 (6:23)	11 (3:22)	<0.001
Subcutaneous fat area (mm^2)	11014 (3019:58246)	13401.5 (1687:36798)	20147 (4962:20147)	18459 (3656:39394)	21938 (8059:43874)	21864 (3280:48729)	<0.001

CT: Computed tomography; HU: Hounsfield unit: Millimeter; mm^2: Millimeter square

ber ratio, anthropometric measurements, visual and quantitative PS, aortic and large vessel calcification, and pancreatic atrophy (Tables 3 and 4).

A positive agreement was observed between the quantitative and visual evaluations (Cohen's kappa coefficient=0.587, p<0.001). In addition, both evaluations had a positive correlation with age, anthropometric measurements, pancreatic atrophy, and aorta and large vessel calcification (p<0.001) (Table 5). A positive correlation was also observed between the presence of short pancreas and quantitative steatosis (r=0.132, p=0.001), but no significant correlation was determined for the visual evaluation of steatosis (p=0.056) (Table 5).No statistically significant correlation was determined between sex, pancreatic calcification, and the results of visual and quantitative steatosis evaluation methods (p=0.659, p=0.549; p=0.258, and p=0.193, respectively) (Table 5). Age was determined to independently increase the risk of PS (odds ratio [OR], 1.80; 95% confidence interval [CI], 1.066:1.095; p<0.001).

DISCUSSION

Currently, the most important tools in the evaluation of PS are radiological methods (4). Although biopsy is the gold standard in steatosis evaluation, because of the location of the pancreas, risk of complications, and sampling bias, the radiological methods still present as better non-invasive alternatives (22). Transabdominal ultrasound is not sufficient for a quantitative evaluation and has other limitations because of the localization of the pancreas (5, 22). However, endoscopic ultrasound (EUS) is the best alternative for cross-sectional imaging for the pancreas. In a recent study by Lesmana et al. (23), the authors concluded that EUS could be considered a screening tool for the early detection of pancreatic cancer in PS. MRI provides both quantitative and qualitative information for the evaluation of PS. However, the visceral fat tissue around the pancreas, small size of the pancreas, and irregular parenchymal structure make MRI images vulnerable to chemical shift artifacts (24). Although MRI-based techniques provide accurate results in the evaluation of fatty liver, the factors mentioned create errors and dif-

Table 5. Correlations of visual and quantitative pancreatic steatosis evaluations with different parameters.

Parameters		Visual pancreatic steatosis	Quantitative pancreatic steatosis
Sex	rh	−0.018	−0.024
	p	0.659	0.549
Age	rh	0.445	0.514
	p	<0.001	<0.001
Pancreatic calcification	rh	−0.045	0.052
	p	0.258	0.193
Visual pancreatic atrophy	rh	0.197	0.483
	p	<0.001	<0.001
Short pancreas	rh	0.076	0.132
	p	0.056	0.001
Visual visceral fat	rh	0.323	0.308
	p	<0.001	<0.001
Aortic and large vessel calcification	rh	0.418	0.386
	p	<0.001	<0.001
AP diameter	rh	0.345	0.339
	p	<0.001	<0.001
Transverse diameter	rh	0.410	0.387
	p	<0.001	<0.001
Abdominal circumference	rh	0.410	0.395
	p	<0.001	<0.001
Anterior subcutaneous fat diameter	rh	0.175	0.149
	p	<0.001	<0.001
Posterolateral subcutaneous fat diameter	rh	0.233	0.232
	p	<0.001	<0.001
Intra-abdominal fat diameter	rh	0.262	0.190
	p	<0.001	<0.001
Posterior subcutaneous fat diameter	rh	0.261	0.264
	p	<0.001	<0.001
Subcutaneous fat area	rh	0.296	0.289
	p	<0.001	<0.001

AP: Anterior-posterior; rh: Spearman's rho correlation coefficient

ficulties in pancreatic evaluation. In recent literature, like liver fat quantification, histopathological and non-contrast CT correlated MRI-based quantitative methods, such as PDFF, have been used in PS (24,25). Compared with the other methods, CT has come to the forefront as a practical and readily available modality, providing both qualitative and quantitative evaluations in a short time without using contrast agents (5, 24).

Fat accumulation in the pancreas is a general term used for fatty pancreas, PS, and pancreatic lipomatosis (4). PS and fatty pancreas are the most preferred terms in recent literature. In this study, we investigated pancreatic fat accumulation in the pancreas. Although PS is a subject of interest, there are only a few studies in the literature investigating its prevalence. In a study by Wong et al. (25), the prevalence of PS was determined as 16.1% in a healthy population using MRI, and a cutoff value of 10.4% was reported. Another result emerging from the study in the literature is that there could be a certain rate of natural steatosis in the pancreas of a healthy group. Therefore, in asymptomatic individuals, incidentally, detected minimal PS may not be clinically important. A previous study determined minimal PS in patients with grade 1 NAFLD (26). A study of 1,190 patients in China reported the PS prevalence as 30.7% using transabdominal ultrasound, and it was more frequently seen in men than women (27). In our study, using non-contrast CT, the prevalence rates of both quantitative and visual steatosis evaluations were similar to those of the Chinese study. However, unlike the Chinese study, we did not find any statistically significant difference between the sexes with respect to steatosis prevalence.

Although various non-contrast CT criteria are used in the evaluation of fatty liver, there are no widely accepted specific criteria or cutoff values for PS. In a study by Kim et al. (24), CT attenuation markers were found to have a statistically significant relationship with histological steatosis grade and impaired glucose tolerance but not with the visceral fat tissue area. In the same study, a statistically significant correlation was determined between the pancreas minus spleen (P−S) and pancreas/spleen (P/S) CT number markers and intrapancreatic histological grade (24). A recent study calculated satisfactory sensitivity (0.79) and specificity (0.79) rates in receiver operating characteristics analysis when the cutoff value was accepted as a 0.7 ratio of the mean pancreatic/mean splenic CT number (19). Takahashi et al. (28) and Hori et al. (29) reported that the area- and attenuation-based measurement of the pancreatic fat by CT showed correlation with the histopathology-based assessment. This study found that the prevalence of PS at a cutoff value of 0.7 determined in the quantitative PS evaluation posi-

tively correlated with the prevalence value obtained from the visual evaluation.

In the quantitative evaluation, although PS was observed to be more diffuse in the 3 anatomic regions, the tail section was the area of most steatosis. Therefore, we suggest that the sections of the pancreas, especially the tail section, should be assessed using area- or attenuation-based methods via CT before pancreatoduodenectomy. A previous non-contrast CT study revealed that the CT number of the pancreatic tail was a good predictor of POPF after pancreatoduodenectomy and had a correlation with the acinar cell CT number of the pancreatic resection margin (30). In this study, the visual evaluation revealed that the vast majority ofpatients had none to mild steatosis, and moderate to severe steatosis was detected in 7.8% of men and 9.9% of women. To the best of our knowledge, no specific cutoff value is given in the literature for quantitative grading; therefore, in this study, visual grading was performed by 2 experienced radiologists.

Pancreatic fat content has been reported to be closely related to increased body mass index (BMI), obesity, insulin resistance, metabolic syndrome, and hepatic fat content (22, 27). In an autopsy study by Ogilvie (1), pancreas fat rate was reported to be 17% in obese cadavers and 9% in lean cadavers. Geraghty et al. (31) calculated BMI values and determined various measurement parameters on CT, including AP transverse abdominal measurement, subcutaneous tissue measurements, subcutaneous fat tissue area, and abdominal circumference, and reported a correlation between the predicted and actual BMI values. In another study (32), a relationship was found between obesity and the anterior, posterior, posterolateral, and subcutaneous fat tissue thicknesses and the intra-abdominal fat tissue thickness. In this study, the CT measurement parameters defined in the literature to determine BMI were used with the exception of the intra-abdominal fat tissue thickness and visceral fat tissue, and a statistically significant difference was determined between sexes in terms of all investigated CT parameters.

Comparison of age groups showed that there were significant differences in the anthropometric measurements, and a positive correlation was determined between the measurements obtained from the quantitative and visual steatosis evaluations. Relatively more aortic and larger vessel calcification was observed in men, but this was not statistically significant. Nevertheless, a positive relationship was determined between PS and vascular calcification and pancreatic atrophy.

We found a positive correlation between age and PS, which supported the results of the autopsy studies of Olsen and Stamm (2, 3). Regression analysis in our study determined age as an independent risk factor, increasing the risk of PS by 1.80 folds (95% CI, 1.066:1.095; p<0.001).

Our study had some limitations. It was a retrospective study and inter-observer reliability calculations were not performed. Furthermore, clinical findings, such as diabetes, smoking, and drinking, and more importantly histopathological correlations were not assessed. However, it was easy to calculate the pancreatic/splenic CT number on non-contrast CT; therefore, the results obtained from this modality are reproducible and repeatable for other researchers. Further research is required to compare and correlate different radiological modalities and EUS in PS assessment with clinical features. There is also a need for further retrospective or prospective studies with larger samples to investigate both laboratory and clinical findings.

In conclusion, by evaluating anthropometric measurements together with PS on CT, the results of this study provide the first prevalence rates of PS in Turkey. We believe that radiologists and clinicians need to collaborate to elucidate the issues that remain unclear or conflicting in PS.

Ethics Committee Approval: Ethics committee approval was received for this study from the Ethics Committee of Erzincan University School of Medicine (13.02.2018/19/15).

Informed Consent: Informed consent is not necessary due to the retrospective nature of this study.

Peer-review: Externally peer-reviewed.

Author Contributions: Concept – U.K., O.T.; Design - U.K., O.T.; Supervision - U.K., O.T.; Resource - U.K., O.T.; Materials - U.K., O.T.; Data Collection and/or Processing - U.K., O.T.; Analysis and/or Interpretation - U.K., O.T.; Literature Search - U.K., O.T.; Writing - U.K., O.T.; Critical Reviews - U.K., O.T.

Conflict of Interest: The authors have no conflict of interest to declare.

Financial Disclosure: The authors declared that this study has received no financial support.

REFERENCES

1. Ogilvie RF. The islands of Langerhans in 19 cases of obesity. The Journal of Pathology and Bacteriology 1933; 37: 473-81. [Crossref]
2. Olsen TS. Lipomatosis of the pancreas in autopsy material and its relation to age and overweight. Acta Pathol Microbiol Scand A 1978; 86a: 367-73. [Crossref]

3. Stamm BH. Incidence and diagnostic significance of minor pathologic changes in the adult pancreas at autopsy: a systematic study of 112 autopsies in patients without known pancreatic disease. Hum Pathol 1984; 15: 677-83. [Crossref]
4. Smits MM, van Geenen EJ. The clinical significance of pancreatic steatosis. Nat Rev Gastroenterol Hepatol 2011; 8: 169-77. [Crossref]
5. Alempijevic T, Dragasevic S, Zec S, Popovic D, Milosavljevic T. Non-alcoholic fatty pancreas disease. Postgrad Med J 2017; 93: 226-30. [Crossref]
6. Hori M, Takahashi M, Hiraoka N, et al. Association of pancreatic Fatty infiltration with pancreatic ductal adenocarcinoma. Clin Transl Gastroenterol 2014; 5: e53. [Crossref]
7. Mathur A, Pitt HA, Marine M, et al. Fatty pancreas: a factor in postoperative pancreatic fistula. Ann Surg 2007; 246: 1058-64. [Crossref]
8. Idilman IS, Aniktar H, Idilman R, et al. Hepatic steatosis: quantification by proton density fat fraction with MR imaging versus liver biopsy. Radiology 2013; 267: 767-75. [Crossref]
9. Pickhardt PJ, Graffy PM, Reeder SB, Hernando D, Li K. Quantification of Liver Fat Content With Unenhanced MDCT: Phantom and Clinical Correlation With MRI Proton Density Fat Fraction. Am J Roentgenol 2018; 211: 151-7. [Crossref]
10. Graffy PM, Sandfort V, Summers RM, Pickhardt PJ. Automated Liver Fat Quantification at Nonenhanced Abdominal CT for Population-based Steatosis Assessment. Radiology 2019; 293: 334-42. [Crossref]
11. Chouhan MD, Firmin L, Read S, Amin Z, Taylor SA. Quantitative pancreatic MRI: a pathology-based review. Br J Radiol 2019; 92: 20180941. [Crossref]
12. Koc U, Taydas O. Investigation of the relationship between fatty pancreas and cholecystectomy using noncontrast computed tomography. J Med Imaging Radiat Sci 2019; 50: 220-6. [Crossref]
13. Koc U, Ocakoglu G, Algın O. The Efficacy of the 3-dimensional VIBE-CAIPIRINHA-Dixon technique in the Evaluation of Pancreatic Steatosis. Turk J Med Sci 2020; 50: 184-94.
14. Tahtaci M, Algin O, Karakan T, et al. Can pancreatic steatosis affect exocrine functions of pancreas? Turk J Gastroenterol 2018; 29: 588-94. [Crossref]
15. Miyake H, Sakagami J, Yasuda H, et al. Association of fatty pancreas with pancreatic endocrine and exocrine function. PLoS One 2018; 13: e0209448. [Crossref]
16. Della Corte C, Mosca A, Majo F, et al. Nonalcoholic fatty pancreas disease and Nonalcoholic fatty liver disease: more than ectopic fat. Clin Endocrinol (Oxf) 2015; 83: 656-62. [Crossref]
17. Kaya E, Yilmaz Y. Non-alcoholic fatty liver disease: A growing public health problem in Turkey. Turk J Gastroenterol 2019; 30: 865-71. [Crossref]
18. Yilmaz Y, Kani HT, Demirtas CO, et al. Growing burden of nonalcoholic fatty liver disease in Turkey: A single-center experience. Turk J Gastroenterol 2019; 30: 892-8. [Crossref]
19. Fukuda Y, Yamada D, Eguchi H, et al. CT Density in the Pancreas is a Promising Imaging Predictor for Pancreatic Ductal Adenocarcinoma. Ann Surg Oncol 2017; 24: 2762-9. [Crossref]
20. Saisho Y, Butler AE, Meier JJ, et al. Pancreas volumes in humans from birth to age one hundred taking into account sex, obesity, and presence of type-2 diabetes. Clin Anat 2007; 20: 933-42. [Crossref]
21. Chantarojanasiri T, Hirooka Y, Ratanachu-Ek T, Kawashima H, Ohno E, Goto H. Evolution of pancreas in aging: degenerative variation or early changes of disease? J Med Ultrason 2015; 42: 177-83. [Crossref]
22. Tariq H, Nayudu S, Akella S, Glandt M, Chilimuri S. Non-Alcoholic Fatty Pancreatic Disease: A Review of Literature. Gastroenterology Res 2016; 9: 87-91. [Crossref]
23. Lesmana CRA, Gani RA, Lesmana LA. Non-alcoholic fatty pancreas disease (NAFPD) as risk factor for pancreatic cancer based on endoscopic ultrasound (EUS) examination: a single center experience. JGH Open 2017; 152: 4-7. [Crossref]
24. Kim SY, Kim H, Cho JY, et al. Quantitative assessment of pancreatic fat by using unenhanced CT: pathologic correlation and clinical implications. Radiology 2014; 271: 104-12. [Crossref]
25. Wong VW, Wong GL, Yeung DK, et al. Fatty pancreas, insulin resistance, and beta-cell function: a population study using fat-water magnetic resonance imaging. Am J Gastroenterol 2014; 109: 589-97. [Crossref]
26. Patel NS, Peterson MR, Brenner DA, Heba E, Sirlin C, Loomba R. Association between novel MRI-estimated pancreatic fat and liver histology-determined steatosis and fibrosis in non-alcoholic fatty liver disease. Aliment Pharmacol Ther 2013; 37: 630-9. [Crossref]
27. Zhou J, Li ML, Zhang DD, et al. The correlation between pancreatic steatosis and metabolic syndrome in a Chinese population. Pancreatology 2016; 16: 578-83. [Crossref]
28. Takahashi M, Hori M, Ishigamori R, Mutoh M, Imai T, Nakagama H. Fatty pancreas: A possible risk factor for pancreatic cancer in animals and humans. Cancer Sci 2018; 109: 3013-23. [Crossref]
29. Hori M, Onaya H, Hiraoka N, et al. Evaluation of the degree of pancreatic fatty infiltration by area-based assessment of CT images: comparison with histopathology-based and CT attenuation index-based assessments. Jpn J Radiol 2016; 34: 667-76. [Crossref]
30. Nahm CB, Lui I, Naidoo CS, et al. Density and enhancement of the pancreatic tail on computer tomography predicts acinar score and pancreatic fistula after pancreatoduodenectomy. HPB (Oxford) 2019; 21: 604-11. [Crossref]
31. Geraghty EM, Boone JM. Determination of height, weight, body mass index, and body surface area with a single abdominal CT image. Radiology 2003; 228: 857-63. [Crossref]
32. Gaba RC, Knuttinen MG, Brodsky TR, et al. Hepatic steatosis: correlations of body mass index, CT fat measurements, and liver density with biopsy results. Diagn Interv Radiol 2012; 18: 282-7. [Crossref]